Optical homodyne measurements and entangled coherent states

B.C. Sanders[1,2,*] K. S. Lee,[1,†] and M. S. Kim[1,‡]
[1] *Physics Department, Sogang University, CPO Box 1142, Seoul, 100-611, Korea*
[2] *School of Mathematics, Physics, Computing and Electronics, Macquarie University, New South Wales 2109, Australia*
(Received 21 October 1994; revised manuscript received 3 March 1995)

We show that optical homodyne measurements of coherent states, and of superpositions of coherent states, can be described using the joint photon-number distribution for entangled coherent states. The quadrature-phase distribution interference fringes for superpositions of macroscopically distinct coherent states (the so-called "Schrödinger cat states") are shown to arise from interference in the photon-number distribution for entangled coherent states. The entangled squeezed states are introduced here as squeezed superposition states which are optically mixed with an antisqueezed coherent local oscillator field (squeezing in the other quadrature) at a beam splitter, and we discuss the connection between entangled squeezed states and squeezed-state homodyne detection of squeezed light. Finally the relationship between interference in phase space and fringes in the joint photon-number distribution for the entangled squeezed state is explored.

PACS number(s): 42.50.Dv, 42.50.Ar, 03.65.Bz

I. INTRODUCTION

The superposition principle of quantum mechanics is at the heart of the mystery of quantum theory, and Schrödinger's cat paradox [1] illustrates the conceptual difficulties with extending the superposition principle to the macroscopic world. Consequently much interest has focused on generating and detecting the optical manifestation of the so-called "cat state" by producing a superposition of two macroscopically distinct coherent states [2–5], distinct SU(2) coherent states [6], distinct squeezed states [4,7,8], and distinct phase states [9]. The accepted signature for identifying the existence of a "cat state" is the presence of interference fringes in a homodyne measurement for particular choices of local oscillator phases [3,4]. These fringes are characteristic of the superposition principle and do not arise for a mixture of coherent states.

Two-system entanglement [10] allows more diverse measurement schemes which can admit tests of local realism. An extension of Schrödinger cat states to two-system entanglements of coherent states [11–13] expands the interest in macroscopic superposition states into a realm where a variety of tests can be made. Although measurements including conditional measurements on one mode [11], joint photon-number distribution measurements [12], and Bell inequality tests [11,14] have been studied, a definitive signature of coherent state entanglement, analogous to the signature of the cat state, has not been identified. In this study we identify the joint photon-number distribution as a natural measurement for determining the presence of the entangled coherent state.

Interference fringes in the photon-number distribution are the signature of entanglement, and can be viewed as arising due to interference in phase space [15–17]. Furthermore, the optical homodyne detection [18] of single-mode states is obtained by reducing this joint photon-number distribution to the photon-number difference distribution [19–21], and the interference fringes in the photon-number difference distribution are the source of the well-known fringes in the quadrature-phase distribution for superpositions of distinct states.

A squeezed local oscillator can be introduced in homodyne detection and it is interesting to consider the mixing of a squeezed local oscillator at a beam splitter with a superposition of two distinct "antisqueezed" (squeezing in the other quadrature) coherent states. The fringes in the joint photon-number distribution persist for the incoherent mixture of strongly squeezed states; the nature of this interference and interference in two-dimensional phase space [15,16] is discussed. The reduction of the joint photon-number distribution to the quadrature-phase measurement case is also considered. Of particular interest is the very strong squeezing case which exhibits features somewhat different from the coherent state local oscillator case.

II. OPTICAL HOMODYNE DETECTION

Optical homodyne detection [18,19] can be modeled as the mixing of a local oscillator field, which could be a coherent or a squeezed state of light [19], with a signal field at a beam splitter, and involves joint photon-number distribution measurements of the two output ports of the mixing beam splitter. The signal field mode is represented by mode a and the local oscillator field mode is

*Electronic address: barry@mpce.mq.edu.au
†Present address: Korea Atomic and Energy Research Institute, Daeduk Science Town P.O. Box 7, Daejon, Korea.
‡Electronic address: mshkim@ccs.sogang.ac.kr

represented by b, and the corresponding annihilation operators for the quantized field modes are $\hat{a}$ and $\hat{b}$, respectively. The two outputs are represented by c and d with corresponding annihilation operators $\hat{c}$ and $\hat{d}$. The output field operators are related to the beam splitter input fields by the transformation

$$\hat{B}\begin{pmatrix}\hat{a}\\ \hat{b}\end{pmatrix}\hat{B}^{\dagger}=\frac{1}{\sqrt{2}}\begin{pmatrix}\hat{a}-i\hat{b}\\ \hat{b}-i\hat{a}\end{pmatrix}=\begin{pmatrix}\hat{c}\\ \hat{d}\end{pmatrix} \tag{2.1}$$

for

$$\hat{B}=\exp\left[i\pi(\hat{a}^{\dagger}\hat{b}+\hat{a}\hat{b}^{\dagger})/4\right], \tag{2.2}$$

the unitary beam splitter operator for a 50:50 beam splitter [20].

Optical homodyne detection corresponds to a difference photon counting of the two output fields from the beam splitter. An arbitrarily weighted photodifference count corresponds to a measurement of the operator

$$\mu\hat{c}^{\dagger}\hat{c}-\nu\hat{d}^{\dagger}\hat{d}. \tag{2.3}$$

For $\mu=0$ or $\nu=0$, the photons in only one output port are detected and, for a strong local oscillator, the photon-number distribution can be normalized to produce the desired quadrature-phase measurement. Balanced homodyne detection corresponds to the difference measurement $\mu=\nu$ in (2.3) and directly produces the quadrature-phase measurement for a strong local oscillator field [19]. If an input signal state with density matrix $\hat{\rho}_a$ mixes with a pure local oscillator state $|\Psi\rangle_b$ the photon-number distribution is

$$P_{cd}(m,n)={}_{cd}\langle m,n|\hat{\rho}_{cd}|m,n\rangle_{cd}, \tag{2.4}$$

for the output state

$$\hat{\rho}_{cd}=\hat{B}\hat{\rho}_a\otimes[|\Psi\rangle_b\langle\Psi|]\,\hat{B}^{\dagger} \tag{2.5}$$

and

$$|m,n\rangle_{cd}\equiv\frac{(\hat{c}^{\dagger})^m}{\sqrt{m!}}\frac{(\hat{d}^{\dagger})^n}{\sqrt{n!}}|0\rangle_{cd} \tag{2.6}$$

the two-mode number state. The distribution $P_{cd}(m,n)$ generates the moments for the arbitrary number difference operator (2.3).

The signal input field state is assigned the density operator $\hat{\rho}_a$ and we restrict our attention to the special case that the state consists of a coherent superposition or incoherent mixture of squeezed coherent states [22]. The squeezed coherent state is written as

$$|\alpha,\zeta\rangle_a=\hat{D}_a(\alpha)\hat{S}_a(\zeta)|0\rangle_a \tag{2.7}$$

where the unitary operator $\hat{D}$ is the displacement operator

$$\hat{D}_a(\alpha)=\exp\left(\alpha\hat{a}^{\dagger}-\alpha^{*}\hat{a}\right), \tag{2.8}$$

and $\hat{S}_a(\zeta)$ is the squeezing operator

$$\hat{S}_a(\zeta)=\exp\left\{\left(\zeta\hat{a}^2-\zeta^{*}\hat{a}^{\dagger 2}\right)/2\right\}. \tag{2.9}$$

The coherent state is, in the standard notation, $|\alpha\rangle\equiv|\alpha,\zeta=0\rangle$.

The density operator for the input signal state is

$$\hat{\rho}_a(\alpha,\zeta;\eta)=\hat{\rho}_a^{\rm mix}(\alpha,\zeta)+\eta\hat{\rho}_a^{\rm int}(\alpha,\zeta) \tag{2.10}$$

for

$$\hat{\rho}_a^{\rm mix}(\alpha,\zeta)=[|\alpha,\zeta\rangle_a\langle\alpha,\zeta|+|-\alpha,\zeta\rangle_a\langle-\alpha,\zeta|]/2 \tag{2.11}$$

the density matrix for the mixed state and

$$\hat{\rho}_a^{\rm int}(\alpha,\zeta)=i[|-\alpha,\zeta\rangle_a\langle\alpha,\zeta|-|\alpha,\zeta\rangle_a\langle-\alpha,\zeta|]/2 \tag{2.12}$$

the interference part of the density matrix. For $\eta=1$ the state is the coherent superposition of macroscopically distinct squeezed coherent states [4,8] and is the more common superpositions of coherent states [2,3] for $\zeta=0$. An incoherent mixture of two squeezed coherent states π out of phase arises in the limit that $\eta\to0$. The local oscillator state is assumed to be a pure squeezed coherent state $|\beta,-\zeta\rangle$ and reduces to the coherent local oscillator for $\zeta=0$.

Given the $P_{cd}(m,n)$ distribution, the result of an ideal homodyne detection measurement is readily calculated. The photon-number difference distribution is [21]

$$P_{c-d}(m-n)=\sum_{m+n=0}^{\infty}P_{cd}(m,n|m-n) \tag{2.13}$$

and converges to the quadrature-phase distribution by choosing a strong coherent local oscillator state and the appropriate local oscillator phase. The mean of the distribution $P_{c-d}(m-n)$ approximates the mean quadrature phase, and the variance of the distribution approximates the variance of the quadrature-phase variable.

III. COHERENT STATES

The signal field state is $\hat{\rho}_a(\alpha,\zeta=0;\eta)$ where α is assumed, without loss of generality, to be real, and there is no squeezing. The local oscillator state is assumed to be in a coherent state with complex amplitude $\beta=|\beta|e^{i\varphi}$, and the local oscillator and the signal state $\hat{\rho}_a$ are mixed at the beam splitter; the output state is then

$$\begin{aligned}\hat{\rho}_{cd}=\frac{1}{2}\big[&|\gamma\rangle_c\langle\gamma|\otimes|\delta\rangle_d\langle\delta|\\&+|i\delta\rangle_c\langle i\delta|\otimes|-i\gamma\rangle_d\langle-i\gamma|\\&+i\eta\big(|i\delta\rangle_c\langle\gamma|\otimes|-i\gamma\rangle_d\langle\delta|\\&-|\gamma\rangle_c\langle i\delta|\otimes|\delta\rangle_d\langle-i\gamma|\big)\big],\end{aligned} \tag{3.1}$$

where

$$\gamma=\frac{1}{\sqrt{2}}(\alpha+i\beta)\qquad\text{and}\qquad\delta=\frac{1}{\sqrt{2}}(i\alpha+\beta). \tag{3.2}$$

For $\eta=1$ the state $\hat{\rho}_{cd}$ can be written as the pure state [11]

$$\hat{\rho}_{cd} = |\Psi\rangle\langle\Psi|, \tag{3.3}$$

where

$$|\Psi\rangle = \frac{1}{\sqrt{2}}(|\gamma\rangle_c|\delta\rangle_d + i|i\delta\rangle_c| - i\gamma\rangle_d), \tag{3.4}$$

which can be shown to violate a Bell inequality [14] as required for entangled states [23]. (For $\eta \neq 1$ the output state is not pure and the Bell inequality as constructed in Ref. [14] does not apply.)

In the following we are going to compare the joint photon-number distributions when the output field is pure ($\eta = 1$) and not pure ($\eta \neq 1$). It is convenient to define the two phase parameters Θ and Φ such that

$$\tan 2\Theta \equiv \frac{2\alpha|\beta|}{|\beta|^2 - \alpha^2}\cos\varphi \tag{3.5}$$

and

$$\cos\Phi \equiv \frac{2\alpha|\beta|}{\alpha^2 + |\beta|^2}\sin\varphi. \tag{3.6}$$

Using these parameters, the general form of the joint photon-number distribution is given by

$$P_{cd}(m,n) = \frac{e^{-(\alpha^2+|\beta|^2)}\left(\left[\alpha^2 + |\beta|^2\right]|\sin\Phi|\right)^{m+n}}{2^{m+n}m!n!} \times\left\{\cosh\left[(m-n)\ln|\tan(\Phi/2)|\right] - \eta\sin\left[2(m-n)\Theta\right]\right\}. \tag{3.7}$$

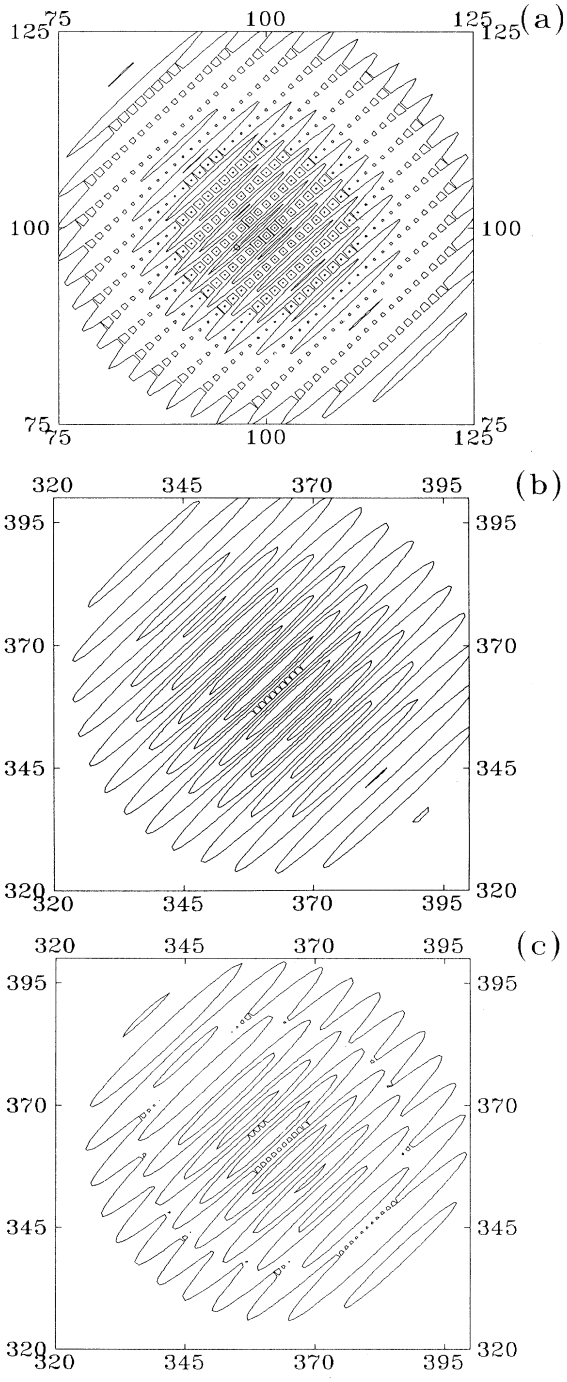

FIG. 1. Contour plot of the joint photon-number distribution $P_{cd}(m,n)$ for the signal field state $\hat{\rho}_a(\alpha = 10, \zeta = 0;\eta)$ and the coherent local oscillator field $|\beta\rangle_b$ for (a) $\beta = 10, \eta = 1$, (b) $\beta = 25, \eta = 1$, and (c) $\beta = 25, \eta = 1/2$. The contour step size is one-fifth the peak height.

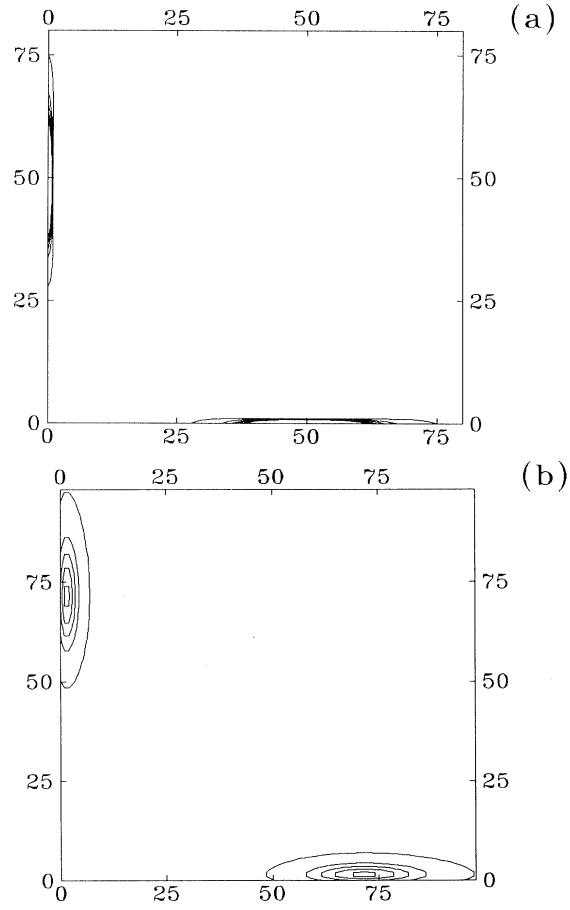

FIG. 2. Contour plot of the joint photon-number distribution $P_{cd}(m,n)$ for the signal field state $\hat{\rho}_a(\alpha = 5, \zeta = 0;\eta)$ and the coherent local oscillator field $|\beta\rangle_b$ for (a) $\beta = 5i, \eta = 1$ and (b) $\beta = 7i, \eta = 1$. The contour step size is one-fifth the peak height.

The oscillatory term in the distribution (3.7), with η as a factor, vanishes for $\eta = 0$ and this case corresponds to the signal field being in an incoherent mixture of product coherent states.

For a local oscillator amplitude β which is purely imaginary, the local oscillator phase is $\varphi = \pi/2$ and the joint photon-number distribution for the output state from the beam splitter reduces to

$$P_{cd}(m,n) = \frac{e^{-(\alpha^2+|\beta|^2)}|\alpha^2 - |\beta|^2|^{m+n}}{2^{m+n}m!n!} \times \cosh\left[(m-n)\ln\frac{|\alpha^2 - |\beta|^2|}{(\alpha + |\beta|)^2}\right] = \frac{1}{2}\left[|\langle m|\gamma\rangle\langle n|\delta\rangle|^2 + |\langle m|\delta\rangle\langle n|\gamma\rangle|^2\right] \quad (3.8)$$

and the distribution (3.8) is independent of η. The photon-number distribution is thus insensitive to the degree of quantum coherence and corresponds to an average of two two-dimensional Poissonian distributions.

If instead the local oscillator has a real amplitude β, then the phase parameter Θ reduces to

$$\Theta = \tan^{-1}\alpha/\beta, \quad (3.9)$$

and the joint photon-number distribution is given by

$$P_{cd}(m,n) = \frac{e^{-(\alpha^2+\beta^2)}\left(\alpha^2+\beta^2\right)^{m+n}}{2^{m+n}m!n!} \times\{1 - \eta\sin[2(m-n)\Theta]\}, \quad (3.10)$$

which may be written as

$$P_{cd}(m,n) = \frac{e^{-(\alpha^2+\beta^2)}\left(\alpha^2+\beta^2\right)^{m+n}}{2^{m+n}m!n!} \times\cos^2[(m-n)\Theta + \pi/4] \quad (3.11)$$

for the pure signal field state of $\eta = 1$. If $\alpha = \pm\beta$, then $\Theta = \pi/4$ and the fringes in the distribution oscillate at the very fine single-photon level. When the field state is pure ($\eta = 1$) and the local oscillator is in phase with the signal field ($\varphi = 0$), the photon-number distribution oscillates as seen in Eqs. (3.5) and (3.8). As the degree of coherence in the entangled states is reduced ($\eta < 1$) or the local oscillator is out of phase with the signal ($\varphi \neq 0$), the oscillations become less pronounced.

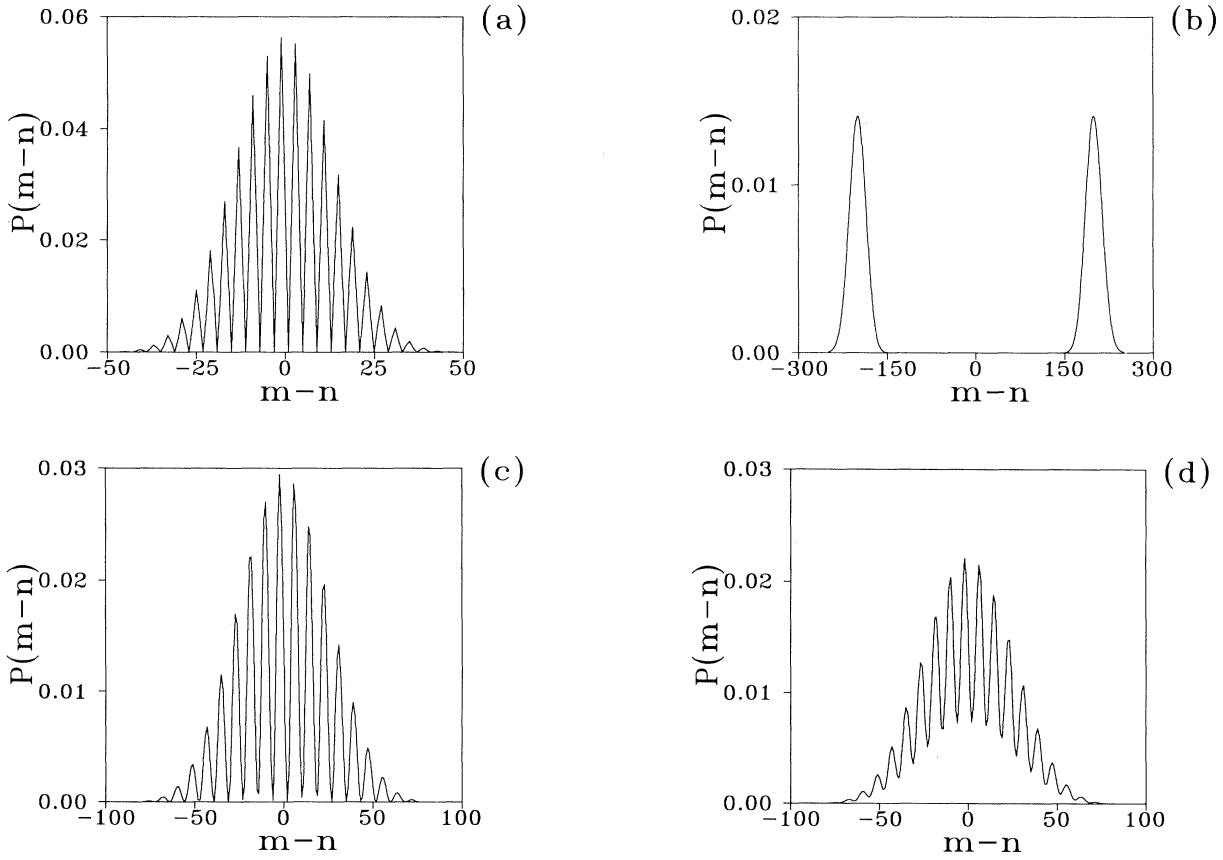

FIG. 3. Graph of the photocount difference distribution $P_{c-d}(m-n)$ for the signal field state $\hat{\rho}_a(\alpha = 10, \zeta = 0; \eta)$ with the coherent local oscillator field $|\beta\rangle_b$ for (a) $\beta = 10, \eta = 1$, (b) $\beta = 10i, \eta = 1$, (c) $\beta = 25, \eta = 1$, and (d) $\beta = 25, \eta = 1/2$. The contour step size is one-fifth the peak height.

The fringes in the joint photon-number distribution are evidence of entanglement and require a judicious choice of local oscillator phase φ to be visible: optimal visibility is attained for $\varphi = 0$ in example (3.11) for $\varphi = 0$ and zero visibility arises for $\varphi = \pi/2$.

The joint photon-number distribution is depicted in Figs. 1(a)–1(c) for the local oscillator state with real amplitude. The degree of quantum coherence η is varied to study the effects on fringe visibility. The fringes are visible in (a) and the very rapid oscillation is due to the fact that $\beta = \alpha$. Actual detection of these fringes would require nearly perfect photodetectors to resolve the fringes to the necessary single-photon level [16]. In (b) the fringes are broader as β is much larger than α. For the case of a signal field which is partially incoherent, the fringes are somewhat diminished by choosing $\eta = 1/2$, as shown in (c), but fringes are still visible. The presence of fringes indicates that entanglement is still present with less than perfect coherence in the two-mode superposition state.

The case of the local oscillator with imaginary amplitude is treated in Figs. 2(a) and 2(b). In (a) the joint photon-number distribution is plotted for $\alpha = |\beta|$ and out of phase by $\pi/2$. The nature of the distribution in (a) corresponds to that for the entanglement of the coherent state with the vacuum state [12]; in (b) the amplitude of the local oscillator amplitude is chosen such that $\alpha \neq \pm|\beta|$.

The photon-number difference distributions corresponding to the parameters of Figs. 1 and 2 are plotted in Figs. 3(a)–3(d). The distributions approximate the quadrature-phase distributions and the granularity is due to the local oscillator field being weak [21]. The choice of a stronger local oscillator in (c) produces smoother distributions compared to that in (a). The fringes in (a) and (c) are the signature for superpositions of macroscopically distinct coherent states using homodyne detection [3]. Fringes are not present in (b) because of the $\pi/2$ phase shift of the local oscillator, and the form of the distribution approaches the double-Gaussian distribution in the limit of a strong local oscillator. The fringes in the photon-number difference distribution (d) are quite diminished for $\eta = 1/2$ but are still evident; the joint photon distribution provides a somewhat clearer signature of entanglement than does the photon-number difference distribution.

IV. SQUEEZED LOCAL OSCILLATOR

A squeezed local oscillator can offer improved sensitivity to interference fringes. The mixing of a superposition of distinct squeezed coherent states, or "squeezed cat" [4], with a squeezed local oscillator is calculated below. The "squeezed cat" is produced by the ideal nonlinear optical Kerr interaction from an initial squeezed state in the same way that a "cat state" is produced from an initial coherent state [3]; the "squeezed cat" state is written as

$$|\Psi\rangle_a = 2^{-1/2}\left[|\alpha,\zeta\rangle_a + i|-\alpha,\zeta\rangle_a\right] \tag{4.1}$$

and the mixed state is represented by the density operator (2.11).

For the pure state $\eta = 1$, and the squeezed coherent local oscillator state $|\beta,-\zeta\rangle_b$, the pure state output from the beam splitter is

$$|2^{-1/2}(\alpha+i\beta),\zeta\rangle_c|2^{-1/2}(i\alpha+\beta),-\zeta\rangle_d + i|2^{-1/2}(-\alpha+i\beta),\zeta\rangle_c|2^{-1/2}(-i\alpha+\beta),-\zeta\rangle_d \tag{4.2}$$

which is an *entangled squeezed coherent state.* The state (4.2) cannot be expressed as a product state for general choices of α, β, and ζ and is therefore entangled; the Schmidt form can be found for entangled squeezed coherent states which exhibit the entanglement quite clearly [14]. The c output is squeezed and the d output is antisqueezed. The entangled coherent states are a special case of the entangled squeezed coherent states (4.2) for $\zeta = 0$.

The mixing of a squeezed coherent local oscillator with

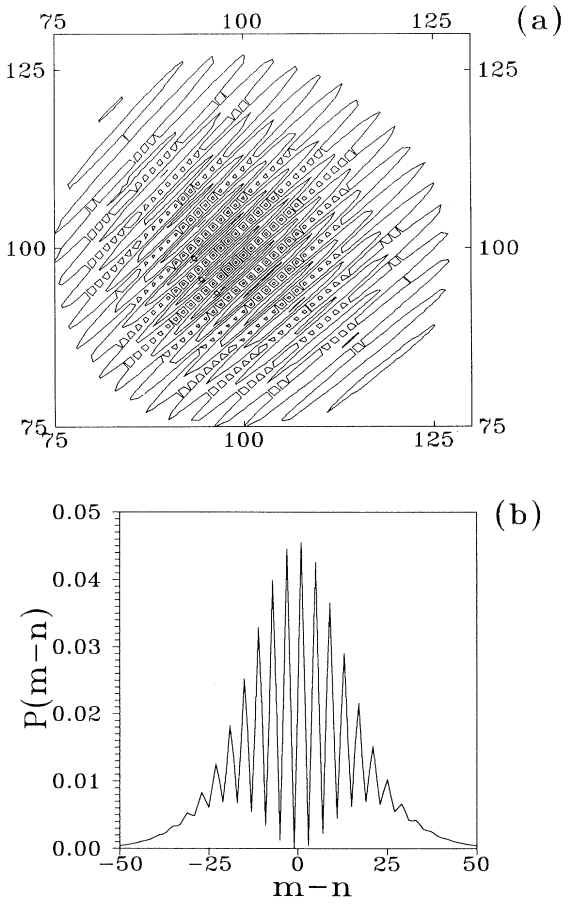

FIG. 4. Contour plot of (a) the joint photon-number distribution $P_{cd}(m,n)$ and (b) the photon-number difference distribution $P_{c-d}(m-n)$ for the signal field state $\hat{\rho}_a(\alpha = 10, \zeta = 0.5; \eta = 1)$ and the squeezed coherent local oscillator field $|\beta = 10, \zeta = -0.5\rangle_b$. The contour step size is one-fifth the peak height.

a "squeezed cat state" (squeezing in the same quadrature) can be considered as well and the resolution of interference fringes in the photon-number difference distribution will be modified (see the discussion below). However, this input state is not considered here as the output state is not an entangled squeezed state. Mixing two squeezed states at a beam splitter will produce a two-mode squeezed output state (for two different spatial modes) [24], but the choice of one squeezed state and one antisqueezed state as beam splitter inputs produces a product output state. We exploit the advantages of mixing squeezed and antisqueezed states at a beam splitter to relate squeezed-state homodyne detection of "squeezed cats" with the entangled coherent states.

In Figs. 4(a) and 4(b) the joint photon-number distributions and the reduced photon-number difference distribution are presented for $\alpha = \beta = 10$, $\zeta = 0.5$, and $\eta = 1$. Interference fringes are visible for the squeezed entangled state as well as for the entangled coherent states. The photon-number difference distribution reveals fringes which are not as clear as for the unsqueezed case. The reason for this reduction in fringe visibility in the difference distribution, and consequently in the quadrature-phase measurement, is due to choosing a squeezed local oscillator for an "anti-squeezed cat." The photodifference measurements reveal good fringes near the center of the distribution, but the fading of the fringes further out is a consequence of the phase space overlap between the local oscillator state and the "squeezed cat" after mixing at the beam splitter. If the "cat" and the local oscillator were squeezed in the same quadrature, then the fringes could be improved.

The joint photon-number distributions and the reduced photon-number difference distribution are presented for the case of very strong squeezing in Figs. 5(a) 5(b), and 6. The degree of squeezing is large in order to show that fringes in the joint photon-number distribution persist even for the incoherent mixture $\eta = 0$ in Fig. 6. The photon-number difference distribution in Fig. 5(b) does not exhibit oscillations due to the strong antisqueezing of the local oscillator with respect to the superposition of the squeezed states. As the local oscillator is strongly antisqueezed, the phase space overlap between the local oscillator and the signal smears out interference fringes. The joint photon-number distribution for $\eta = 0$ is plotted in Fig. 6, but the corresponding photon-number distribution is not plotted because, due to the noisy homodyne detection using squeezed light for an "antisqueezed cat," the distribution does not differ in any noticeable way from the pure state calculation depicted in Fig. 5(b). The distribution fringes are an evidence of phase space interference and the setting of $\eta = 0$, whilst removing the four-dimensional phase space interference, does not remove the two-dimensional interference that produces interference in phase space and fringes in the photon-number distribution for a single-mode squeezed state [15,16]. The fringes are diminished for lower levels

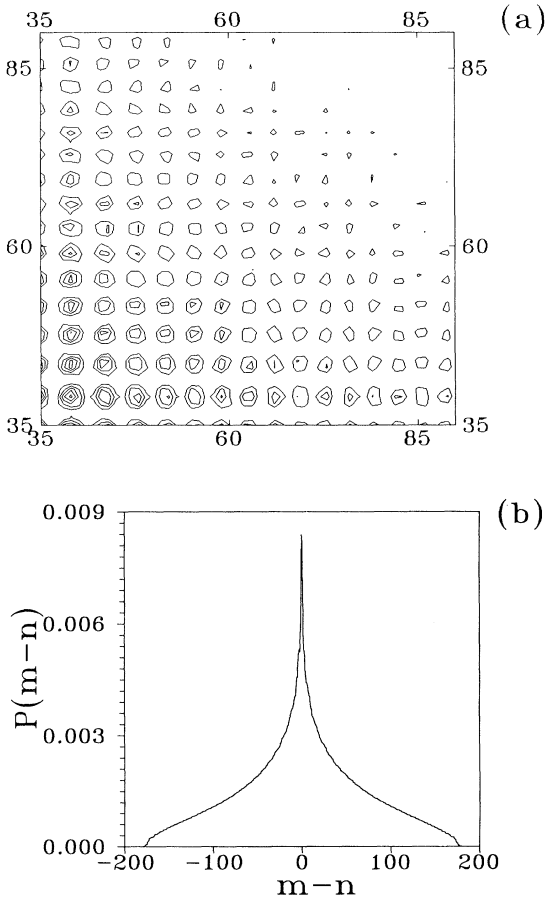

FIG. 5. Contour plot of (a) the joint photon-number distribution $P_{cd}(m,n)$ and (b) the photon-number difference distribution $P_{c-d}(m-n)$ for the signal field state $\hat{\rho}_a(\alpha = 7, \zeta = 3.05; \eta = 1)$ and the squeezed coherent local oscillator field $|\beta = 7, \zeta = -3.05\rangle_b$. The contour step size is one-fifth the peak height.

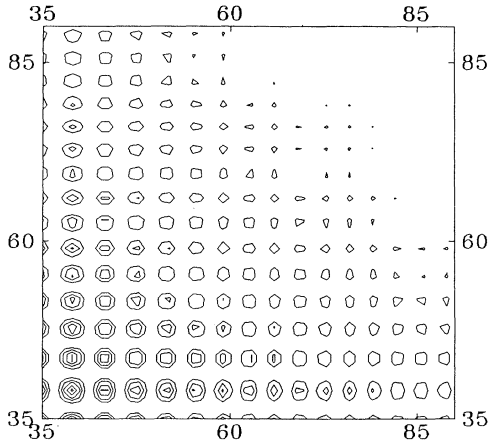

FIG. 6. Contour plot of the joint photon-number distribution $P_{cd}(m,n)$ for the signal field state $\hat{\rho}_a(\alpha = 7, \zeta = 3.05; \eta = 0)$ and the squeezed coherent local oscillator field $|\beta = 7, \zeta = -3.05\rangle_b$. The contour step size is one-fifth the peak height.

of squeezing which corresponds to less prominent two-dimensional phase space interference.

V. CONCLUSIONS

The joint photon-number distribution has been shown to be an important quantity for distinguishing entangled coherent states from mixtures. Moreover, the photon-number difference distribution, which is obtained by reducing the joint photon-number distribution, corresponds to the quadrature-phase measurements of cat states in the limit of a strong local oscillator field. Interference fringes in the two distributions are very much related and the homodyne measurement of "cat states" reveals one aspect of detecting entangled coherent states.

The entangled coherent states are a special case of the entangled squeezed states which have been introduced here and arise if "squeezed cats" are mixed with an anti-squeezed coherent local oscillator field at the beam splitter. The entangled squeezed states present joint photon-number distributions which exhibit interference fringes even for the case that the "squeezed cat" is reduced to an incoherent mixture of squeezed states. The persistence of these interference fringes is a manifestation of two-dimensional phase space interference for each of the component squeezed states.

An important feature of the interference fringes in the joint photon-number distribution is the fine graining of the oscillations. Measurements of the oscillations are thus very difficult with anything but a very high efficiency photodetector. Despite the difficulty in detecting this signature of entanglement, the joint photon-number distribution is the natural distribution to search for effects due to entanglement and these fringes arise for the appropriate choice of local oscillator phase.

ACKNOWLEDGMENTS

This research has been supported by the Australian Academy of Sciences and the Korea Research Foundation through the nondirected research fund project. We are grateful to the Korean Science and Engineering Foundation for a travel grant.

[1] E. Schrödinger, Naturwissenschaften **23**, 812 (1935).
[2] G. J. Milburn, Phys. Rev. A **33**, 674 (1986); **33**, 674 (1986).
[3] B. Yurke and D. Stoler, Phys. Rev. Lett. **57**, 13 (1986).
[4] A. Mecozzi and P. Tombesi, Phys. Rev. Lett. **58**, 1055 (1987); P. Tombesi and A. Mecozzi, J. Opt. Soc. Am. B **4**, 1700 (1987).
[5] M. S. Kim and V. Bužek, Phys. Rev. A **46**, 4239 (1992).
[6] B. C. Sanders, Phys. Rev. A **40**, 2417 (1989).
[7] B. C. Sanders, Phys. Rev. A **39**, 4284 (1989).
[8] G. J. Milburn, A. Mecozzi, and P. Tombesi, J. Mod. Opt. **36**, 1607 (1989).
[9] B. C. Sanders, Phys. Rev. A **45**, 7746 (1992).
[10] M. A. Horne, A. Shimony, and A. Zeilinger, Phys. Rev. Lett. **62**, 2209 (1989).
[11] B. C. Sanders, Phys. Rev. A **45**, 6811 (1992); **46**, 2966 (1992).
[12] B. Wielinga and B. C. Sanders, J. Mod. Opt. **40**, 1923 (1993).
[13] N. A. Ansari and V. I. Man'ko, Phys. Rev. A **50**, 1942 (1994).
[14] A. Mann, B. C. Sanders, and W. J. Munro, Phys. Rev. A **51**, 989 (1995).
[15] W. Schleich and J. A. Wheeler, Nature (London) **326**, 574 (1987); J. Opt. Soc. Am. B **4**, 1715 (1987).
[16] G. J. Milburn and D. F. Walls, Phys. Rev. A **38**, 1087 (1988).
[17] C. M. Caves, C. Zhu, G. J. Milburn, and W. Schleich, Phys. Rev. A **43**, 3854 (1991).
[18] H. P. Yuen and J. H. Shapiro, IEEE Trans. Inf. Theory **24**, 657 (1978); J. H. Shapiro, H. P. Yuen, and J. A. Machado Mata, *ibid.* **25**, 179 (1979); H. P. Yuen and J. H. Shapiro, *ibid.* **26**, 78 (1980).
[19] M. J. Collett, R. Loudon, and C. W. Gardiner, J. Mod. Opt. **34**, 881 (1987).
[20] R. A. Campos, B. E. A. Saleh, and M. C. Teich, Phys. Rev. A **40**, 1371 (1989).
[21] W. K. Lai, V. Bužek, and P. L. Knight, Phys. Rev. A **43**, 6323 (1991).
[22] D. F. Walls, Nature (London) **306**, 141 (1983); R. Loudon and P. L. Knight, J. Mod. Opt. **34**, 709 (1987).
[23] N. Gisin, Phys. Lett. A **154**, 201 (1991).
[24] C. M. Caves and B. L. Schumaker, Phys. Rev. A **31**, 3068 (1985).